lubricants

MDPI

Article

The Study of Mechanical and Tribological Performance of Fulleroid Materials Filled PA 6 Composites

Dmitry V. Pikhurov [1] and Vjacheslav V. Zuev [1,2,*]

[1] University ITMO, Kronverkskiy pr., 49, Sankt Petersburg 197101, Russian; nefaeron@gmail.com
[2] Institute of Macromolecular Compounds of the Russian Academy of Sciences, Bolshoi pr. 31, 199004 Sankt Petersburg, Russian
* Correspondence: zuev@hq.macro.ru; Tel.: +7-812-328-8527; Fax: +7-812-328-6869

Academic Editors: Antolin Hernández Battez and Rubén González Rodríguez
Received: 27 November 2015; Accepted: 14 April 2016; Published: 28 April 2016

Abstract: The effect of fulleroid materials (fullerene C_{60} and fullerene soot which is used for fullerene production) and carbon fibers on the mechanical and tribological properties of polymer nanocomposites based on polyamide 6 (PA6) was investigated. Composites were synthesized by *in situ* polymerization and direct mixing in an extruder. It was found that addition of these fillers during *in situ* polymerization was more effective at improving the mechanical and tribological properties of the composites. The use of the nanoparticles was an effective way to decrease the friction coefficient of the polymer composites because the fillers were the same size as the segments of the surrounding polymer chains. The steady state coefficients of friction with the addition of fulleroid fillers were lower than that of unfilled PA6. The lowest coefficient of friction was observed for PA6 filled with 1 wt. % fullerene soot.

Keywords: composites; manufacturing; mechanical properties; tribology; friction; fullerene C_{60}; fullerene soot

1. Introduction

A number of polymers can be considered to be competitive materials for tribological applications because of their low friction coefficients against steel counterparts, good damping properties, and self-lubricating ability. PA6 has been reported to have a superior sliding wear resistance against a steel counterface relative to other polymers. In order to meet the special needs of tribological applications, polymer composites can be designed by selecting the correct composition and choosing the appropriate manufacturing process. The improvement of mechanical and/or tribological properties of polymers by incorporation of particulate filler materials has been widely studied [1]. Under extreme friction conditions, however, conventional polymer composites are usually not effective for antiwear and friction reduction—for example, under heavy load. The nanoparticle reinforced polymer composites are the most rapidly growing class of materials due to a good combination of high strength and modulus at very low levels of loading [2]. Nanocomposites are compatible with conventional polymer processing, thus avoiding the costly stay up required for the fabrication of conventional fiber-reinforced composites. When the fillers possess dimensions on the order of nanometers, even a small concentration can lead to enhancements in properties, unprecedented in conventional composites [3]. The unique properties of polymer nanocomposites are attributed to the high filler surface area-to-volume ratio, which results in significant interfacial areas of contact between the polymer and the particles. The large interfacial areas of contact enable a substantial fraction of polymer segments to interact directly with the filler particles, even at low particle concentrations. Mechanical and tribological properties of polymer nanocomposites are not as a simple as the addition of individual properties of the components, and depend on many factors and synergetic interactions. A new group of polymer nanocomposites based on integrating fullerene-like fillers into conventional polymer matrix has been developed in the last years. A review of these works is given by Maharaj and Bhushan [4]. Polymer nanocomposites containing fullerenes have great potential for versatile applications which include optical interrupters, polymer photoconductors, electrodes in lithium batteries, electro-optical structures in nano-electronics, nonlinear optics and photovoltaic devices [5,6]. The efforts towards fullerene reinforced composites for practical applications that have been performed by using melt compounding are very limited in the academic field. Fullerene has been used as an additive in several thermoplastic polymers including polyethylene [7], polypropylene [8], polyamide [9] with the melt mixing method. However, new additives look for the reduction of both the friction and wear or required the reduction of lubrication. So far, most research concentrated on self-lubricant composites which have been obtained with the addition of fullerene-like nanoparticles of tungsten disulfide (WS_2) and molybdenum disulfide (MoS_2) to common polymers. These fillers form complex aggregates and are non-monodisperse, which complicates the analysis of the results obtained [10].

Polymer/fullerene C_{60} blends are ideal systems for studying polymer- nanoparticles interactions, since fullerene C_{60} is monodisperse, available in high purity, and dispersible in many polymers and block copolymers [11]. The most challenging problem in the fabrication of polymer nanocomposites is dispersing the nanofillers in the polymer matrix [12]. The nanofillers strongly self-associate into ropes and other highly-ordered structures, which are extremely difficult to disperse in polymers. As result, the mechanical properties of polymer nanocomposites can be very far from predictions [13]. The methods of solution blending, melt blending, latex technology, solid-state shear pulverization, coagulation spinning, and *in situ* polymerization have been widely applied to produce nanofillers/polymer composites [14].

In this work, we have studied the influence of fullerene C_{60} or fullerene C_{60} containing materials and the method of preparations of the nanocomposites on the mechanical properties and tribo-performance of PA 6 based composites. To our best knowledge, this is the first study that investigates the properties of fullerene C_{60} filled PA6 prepared with melt blending method and *in situ* polymerization.

2. Experimental Section

2.1. Material and Manufacturing

Fullerene C60 (purity 99.9%) and fullerene soot containing about 10.5% fullerene, which was supplied by ZAO ILIP (Saint Petersburg, Russia), were used as fillers. The used fullerene soot is an ultra dispersed carbon formed at a voltaic arc of graphite in an inert gas atmosphere during fullerene production, with particle diameters of 0.5–2.0 μm. Carbon fibers (PO Chimvolokno, Svetlogorsk, Belorussia) with fiber length of 400 μm and diameter of 0.2 μm were selected as traditional fillers to enhance the mechanical properties and friction of PA 6 matrix. Plasticizer ARMOSIL E® (AKZO NOBEL (amide of oleic acid)) was added to the 1% C_{60} samples to aid the C_{60} dispersion.

In the first method, the PA6 based polymer composites were obtained by polymerization of a fine mechanical mixture of ε-caprolactam (OAO Kuibishevasot, Samara, Russia), in the amount of 100–220 g, with calculated amounts of filler, using sodium as catalyst and toluene 2,6-diisocyanate as cocatalyst at 140–160 °C for 12 h [15].

In the second method, the granules of PA6 Волгамид® 32, OAO Kuibishevasot, Samara, Russia, here after B32) were premixed with calculated amounts of filler powder for 5 min in a high-speed powder mixer. The composites of PA6 were then prepared by a twin screw extruder in the temperature range 230–250 °C. Finally, all the test specimens of both types of composites were manufactured using an injection molding machine.

2.2. Mechanical Properties

Tensile properties were measured in the accordance with ISO 527. Tests were conducted using 6 × 6 × 40 mm^3 specimens for tensile strength and Young's modulus estimation on a UTS 10 device (UTS Test System, Wolfsburg, Germany) at an elongation rate of 2 mm/min. No less than five specimens were taken for each sample to obtain an average value.

2.3. Friction Testing

Dry sliding tests were conducted on a disc-on-pin friction testing machine MTU-01 (NPO Nanotechnology, Moscow, Russia) (shown in Figure 1).

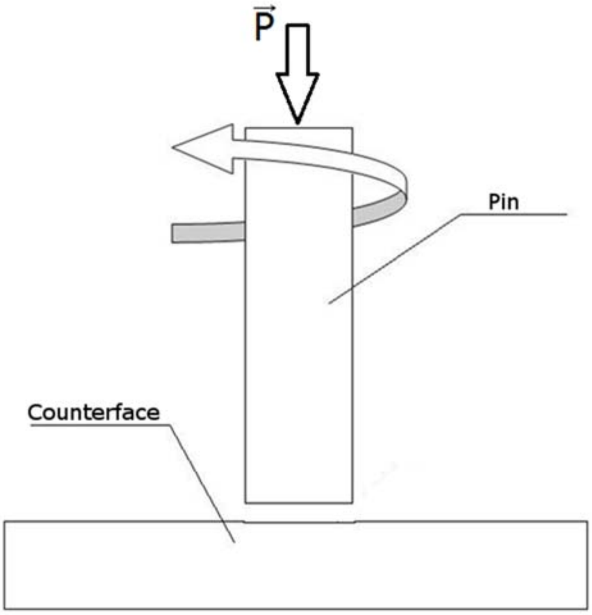

Figure 1. Schematic diagram of friction test rig.

Polymer discs were tested against the cylindrical steel pin (mark 3® (Cherepovez, Russia)), hardness 58HRC, diameter of 19 mm, a surface roughness of 0.11 µm Ra). The sliding conditions were 1 m/s, with a load of 400 N. Each measurement was repeated twice. The friction ratio as a function of time was measured, and its mean value was estimated.

2.4. Optical Microscopy

An optical microscope, Micromed Met 400 (Micromed Met, Moscow, Russia), with magnification up to 400, was used to analyze the worn surfaces of the composites.

2.5. Thermal Properties

Differential scanning calorimetry (DSC) measurements were performed using a Netzsch DSC 204F1 instrument (Netsch, Neudorf, Germany) at a scan rate 10 K/min. The glass transition temperatures and melting points of composites were determined.

2.6. Scanning Electron Microscopy

Scanning electron microscopy (SEM) images were obtained with Zeiss ULTRAplus FEG-SEM instrument (Carl Zeiss, Dresden, Germany) with magnification 2000–40,000. The nanocomposites samples were cryo-fractured from bulk specimens, and the fractured samples were coated with a ~5 nm Pt overlayer to avoid charging during electron irradiation.

3. Results and Discussion

3.1. Mechanical Properties

The reinforcement effect in nanocomposites is very sensitive to the quality of the nanoparticle dispersion [16]. Fabrication methods are overwhelmingly focused on improving nanofillers dispersion because better filler dispersion in the polymer matrices has been found to improve the properties. *In situ* polymerization is generally more effective than other potential methods in dispersing nanofillers in a polymer matrix due to high viscosities of polymer solutions and melts. Furthermore, *in situ* polymerization methods enable covalent bonding between the nanofillers and the polymer matrix by using various reactions to promote compatibilization. On the other hand, mixing in an extruder is more acceptable an industrial way for preparation of polymer composites. This stimulated us to choose both these methods as fabrication techniques for synthesis of PA6/fulleroid materials nanocomposites. Analysis of cryochips by SEM microscope shows that the distribution of fillersis homogeneous in all nanocomposite samples. Figure 2 shows the SEM image of the nanocomposite filled with fullerene soot. As one can see, the soot particles did not aggregate.

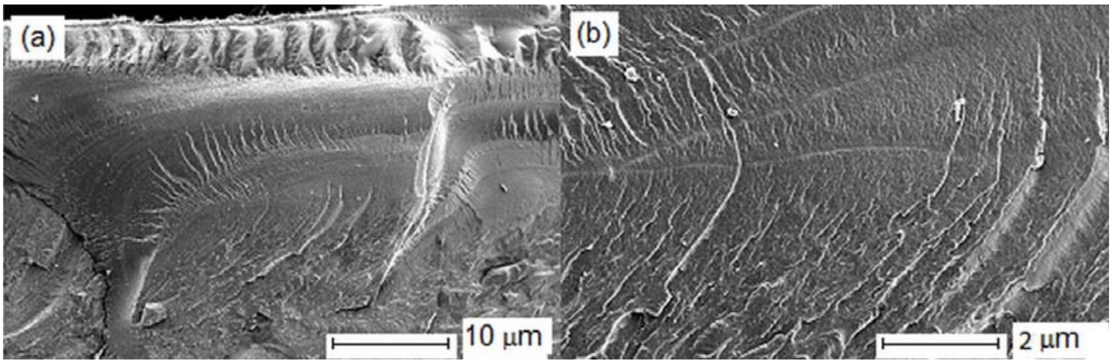

Figure 2. SEM images of fullerene soot/PA6 composite (1 wt. %) at magnification: 2000 (**a**); 10,000 (**b**).

Table 1 shows that Young's modulus and the tensile strength and elongation of the nanocomposites increased slightly at low filler loading, independent of the fabrication method.

Table 1. Effect of loading on the mechanical properties of the polymer nanocomposites.

Loading, wt%	Young's Modulus, GPa	Tensile Strength σ, MPa	Elongation ε, %	Glass Transition, T_g (°C)	Relative Viscosity [d]
Neat PA6 [a]	2.15 ± 0.07	93 ± 5	53 ± 5	85	3.5
B32	0.693 ± 0.017	63 ± 1	290 ± 6	84	3.2
Fullerene C_{60}					
0.01 [a]	2.39 ± 0.12	105 ± 5	58.0 ± 0.5	85	3.4
0.01 [b]	0.714 ± 0.022	65 ± 1	301 ± 6	68	3.2
1 [b,c]	0.265 ± 0.037	11 ± 1	287 ± 2	51	3.2
Fullerene soot					
1 [b]	0.622 ± 0.045	62 ± 1	286 ± 14	55	3.2
Carbon fibers					
10 [a]	3.65 ± 0.1	130 ± 4	24 ± 2	85	3.4

[a] *in situ* polymerization; [b] extrusion with B32; [c] 0.05 wt. % of ARMOSIL E (AKZO NOBEL); [d] 96% H_2SO_4; 1 g of PA6 in 100 mL sulfuric acid.

Furthermore, all of these parameters decreased significantly with increase in filler concentration. This was mainly attributed to the carbon particles aggregating easily as the filler concentration increased. Additionally, the sample with 1% of fullerene C60 also contained ARMOSLIP E (0.05%), which acted as a plasticizer. The difference in properties of neat PA6 synthesized by us and commercial B32 used as the choice of polymer for extrusion was the slightly lower viscosity of B32. The influence of fulleroid materials loading on mechanical properties of PA6 based composites was investigated by us previously [17]. The composites were synthesized by *in situ* polymerization. The mechanical properties of composites were improved by incorporation of the 0.001–1 wt. % fullerene or fullerene soot. The addition of fullerenes into PA6 matrix leads to its selective crystallization only in the α-form crystals that can explain the reinforcement effect of fullerenes. This also explains the absence of dependence of the reinforcement from loading because, if reinforcement was connected with stimulation of selective crystallization by fillers, such an effect should be absent. Similarly, it explains the absence of difference in reinforcement at the loading fullerene C_{60} and fullerene soot. Opposite to these results, the well-known reinforcement at the loading of carbon fibers depends on the amount of fillers. This stimulated us to investigate the tribological behavior of both types of composites.

3.2. Effect of Fillers on Friction

Figures 3–5 show the friction plots for neat PA6 and PA6 filled with different fillers. For all polymer materials, the coefficient of friction starts with a running-in period followed by a steady-state period. It is believed that, within the running-in period, ridges are formed on the surface of the polymer, but within the steady-state period, these ridges disappear and wear debris covers the surface, which leads to lower friction coefficient values. This is typical friction behavior for polymer materials [3].

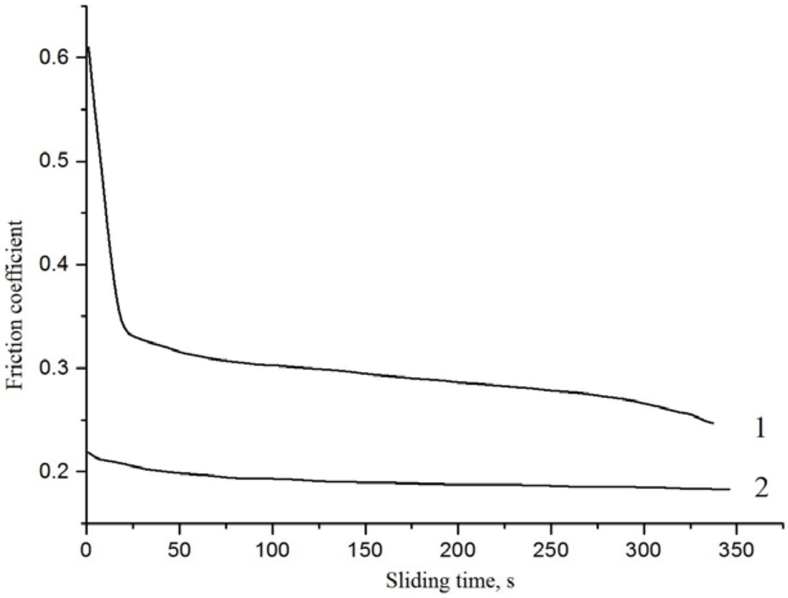

Figure 3. Variation of friction coefficient with sliding time for PA6 obtained by *in situ* polymerization; (1) neat and (2) with 0.01 wt. % of fullerene C_{60}.

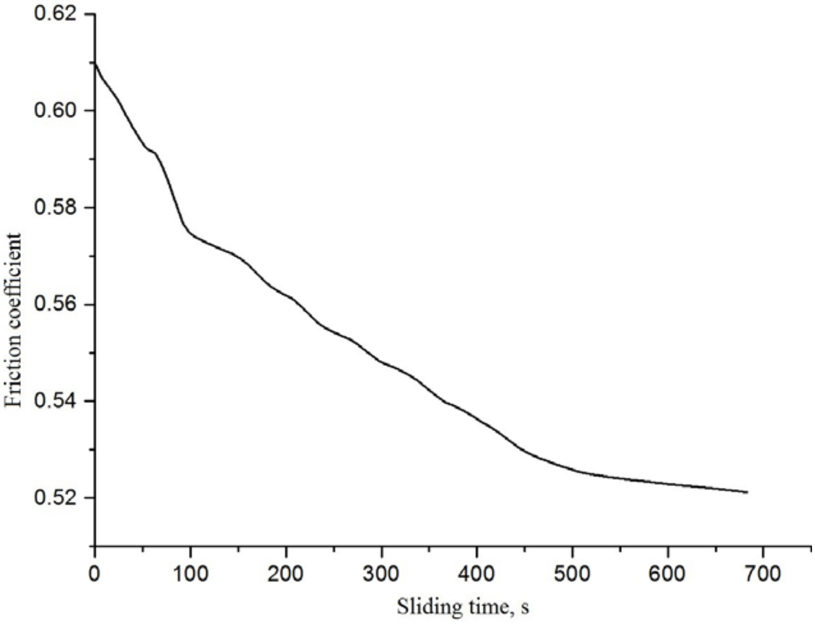

Figure 4. Variation of friction coefficient with sliding time for PA6 obtained by *in situ* polymerization with 10 wt. % of carbon fibers.

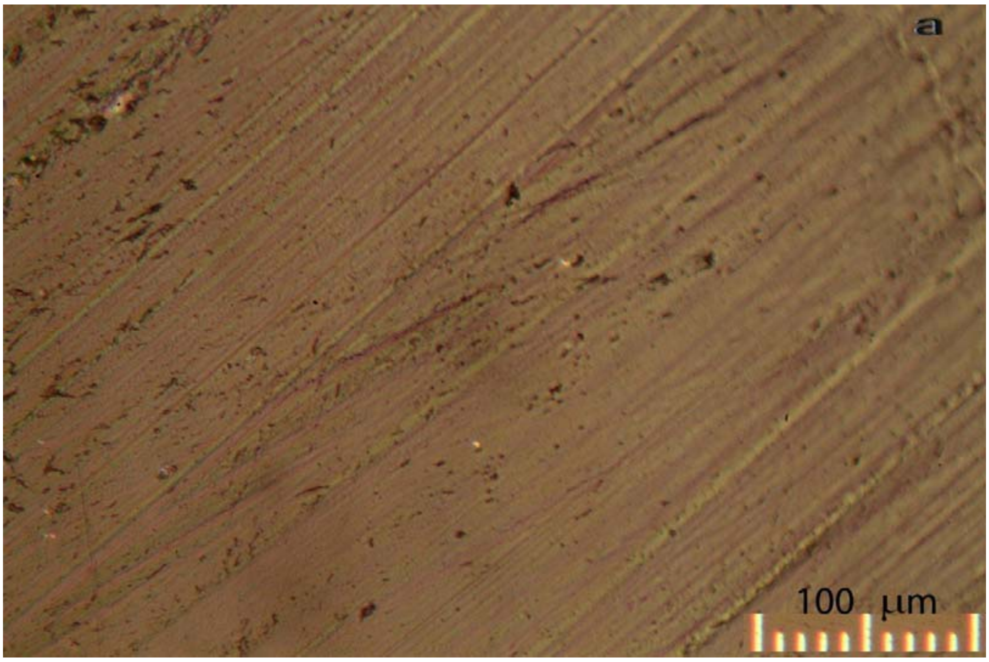

(**a**)

Figure 5. *Cont.*

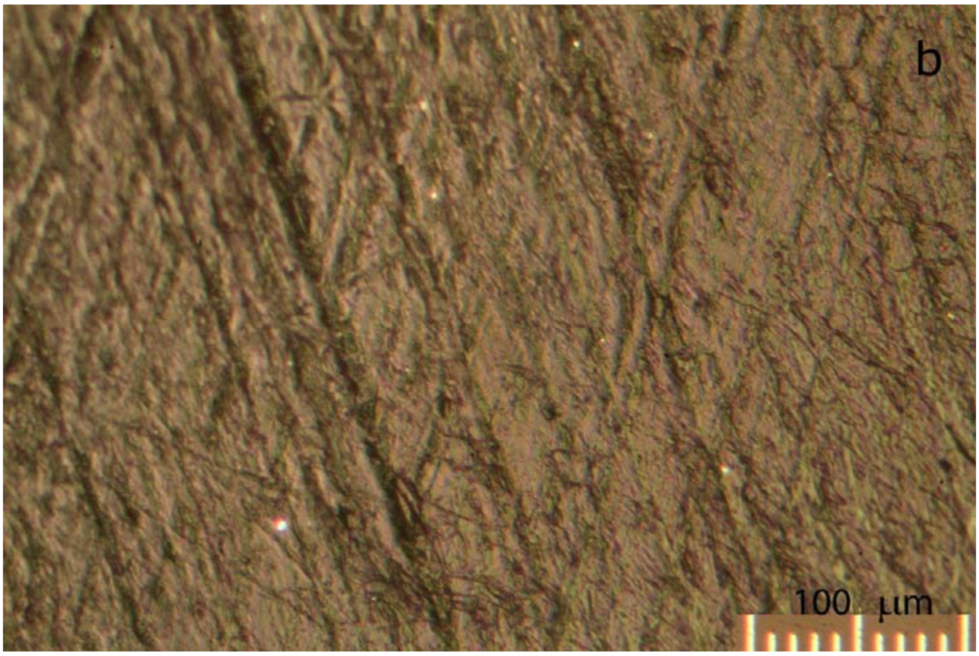

(**b**)

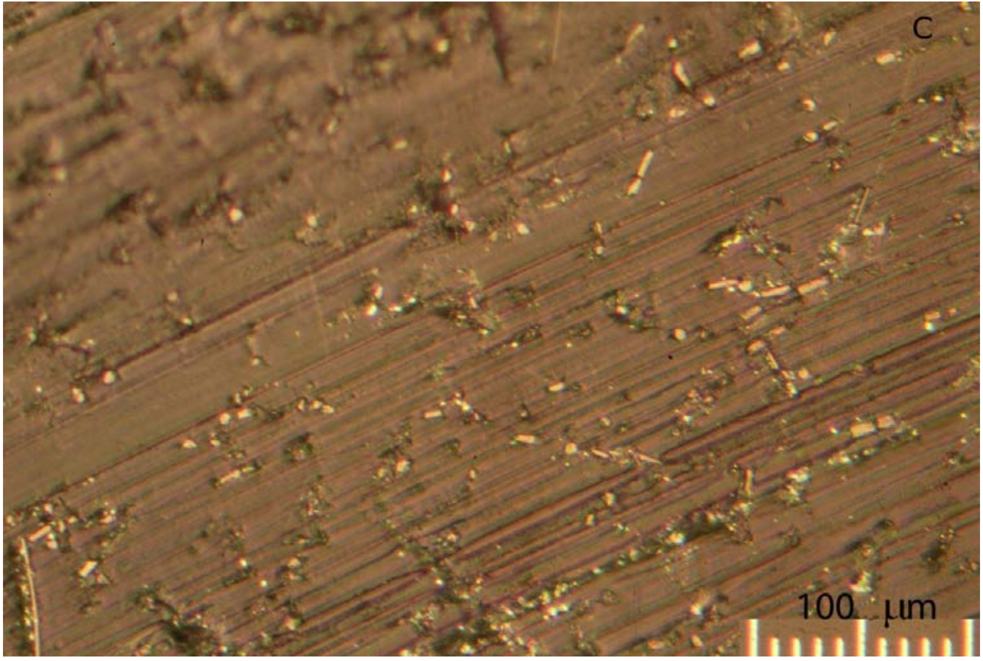

(**c**)

Figure 5. Optical micrographs of worn surfaces of PA6 obtained by *in situ* polymerization: (**a**) neat; (**b**) with 0.01 wt. % of fullerene C_{60}; (**c**) with 10 wt. % of carbon fibers. Magnification 400.

Figure 3 presents the variation of friction coefficients for neat PA6 and PA6 with 0.01 wt. % of fullerene C_{60} both obtained by polymerization *in situ*. The reason for the reduction of the friction coefficient of the composite would be the increase in the Young's modulus. It is a well-known fact that the friction behavior of a polymer composite against a metal is strongly influenced by its ability to form a transfer film on the counterface [18]. The lubricating function of fullerene C_{60} [19] is thought to be responsible for the reduction of the friction coefficient as its composites slide against steel. The fullerene C_{60} forms a thin lubricating film on the counterface, thereby reducing the abrasion process drastically. Both effects combine to the low friction coefficient of the composite compared with neat PA6.

The carbon fiber reinforced PA6 had a Young's modulus higher than that filled by fullerene C_{60} (Table 1). Moreover, as shown in Figure 3, its friction coefficient is also higher.

A lot of papers have been reported on the wear performance of carbon fiber reinforced composites based on polyamides [20,21]. The most probable mechanisms operating in these composites resulting in abrasion and accounting for wear are: fiber-matrix de-bonding, fiber micro-cracking, micro-cutting and micro-pulverization of fibers followed by lifting of the fiber debris and pieces from the matrix, and subsequent removal from the surface, accounting for the wear by leaving behind cavities of appropriate size due to fiber consumption. These proposed mechanisms were supported by optical studies of the worn surfaces (Figure 5). The differences in the worn surfaces were significant. Fiber debris and pieces appeared on the wear scars of the carbon fiber reinforced composite (Figure 5c). For neat PA6 and composites filled with fullerene C_{60}, the worn surfaces were quite smooth. These observations are consistent with the tribological data discussed above. Figure 6 shows the friction plots for the B32 nanocomposites prepared by the twin screw extruder.

The results can be connected to the similar structure of fullerene soot and graphite. Graphite is a good lubricant, which can form a transfer film on a sliding counterpart [22].

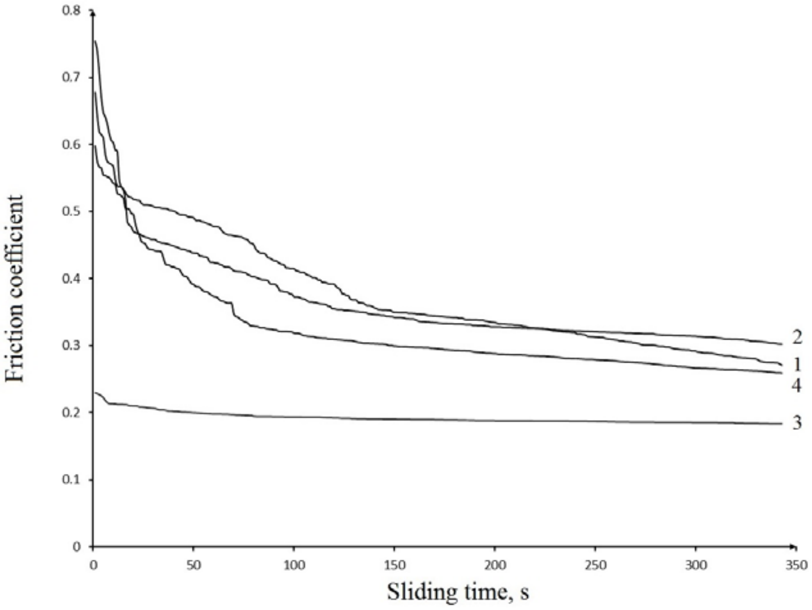

Figure 6. Variation of friction coefficient with sliding time for B32 PA6 obtained by extrusion mixing; (1) neat; (2) with 0.01 wt. % of fullerene C_{60}; (3) with 1 wt. % of fullerene C_{60} and 0.05 wt. % of ARMOSLIP E; (4) with 1 wt. % of fullerene soot.

A similar effect is suggested with the fullerene soot, in combination with the acting of fullerene C_{60} forming part of the soot; it led to the low friction coefficient in B32/fullerene soot sample because the nanoparticles improved the bonding between the transfer film and metallic counterpart [23]. The friction coefficient of the B32 PA6 filled with 0.01 wt. % of fullerene C_{60} prepared by a twin screw extruder was higher than for a composite with 0.01 wt. % of fullerene C_{60} prepared by *in situ* polymerization. This may be connected with lower Young's modulus of the extruder prepared composite.

The highest equilibrium coefficient of friction was observed for the composite filled with 1 wt. % of fullerene C_{60}. The softening of the polymer plays an important role in the friction behavior [24]. As the temperature of worn surface reaches the softening point of the polymer, the adhesive component increases and results in higher coefficient of friction values. Furthermore, the softening for our samples was also evident by the formation of peaks and valleys on worn surfaces. The composite filled with 1 wt. % of fullerene C_{60} also contained 0.05 wt. % of plasticizer ARMOSLIP E. As a result, this composite was soft at room temperature, which leads to a high value of friction coefficient. Figure 7 shows the optical images of worn surfaces of these composites. Beach mark formations can be seen on polymer surface due to composite softening [25]. These beach marks form on-path irregularity on worm surfaces and lead to an increase of friction.

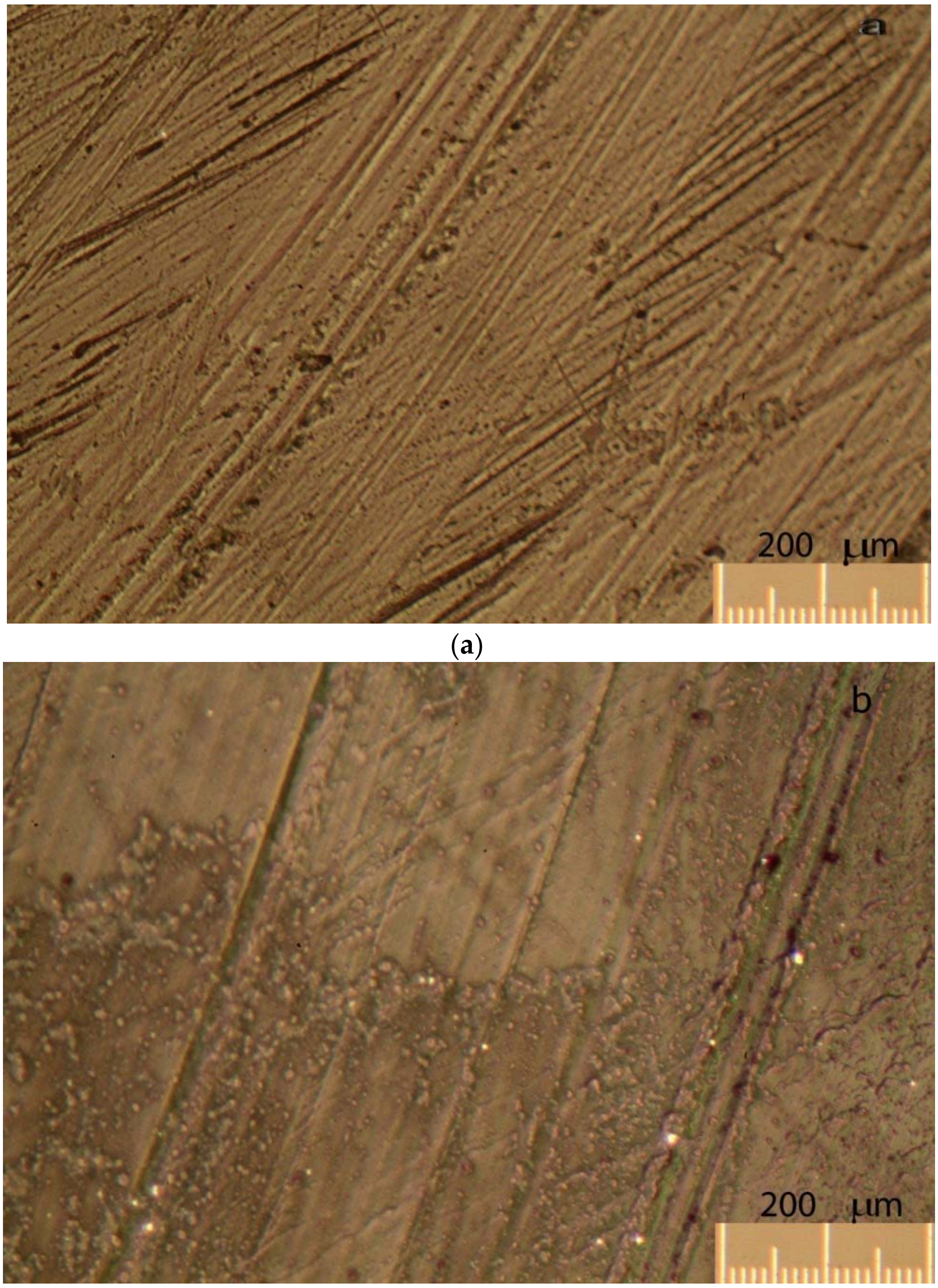

(**a**)

(**b**)

Figure 7. Optical mirographs of worn surfaces of B32 PA6 obtained by extrusion mixing; (**a**) neat; (**b**) with 1 wt. % of fullerene C_{60} and 0.05 wt. % of ARMOSLIP E. Magnification 200.

4. Conclusions

It was concluded that the best way for preparation of the composite with optimal properties is *in situ* polymerization. From the analysis, it was concluded that the mechanical properties and friction performance of PA6 based composite are greatly enhanced by nano reinforcement by fullerene C_{60} at low loading. The reason for the enhancement is the change in phase behavior of polymer matrix (preferably, formation of α-crystalline modification). The resistance to deformation and recovery of the fullerene C_{60} allows them to retain their spherical shape. This leads to lower real area of contact and an increase in the probability for rolling, which facilitates ease of shearing and low friction and wear. It was shown that an increase in concentration of nanofiller up to a minimal level leads to a dramatic fall of the mechanical and friction performance as result of the aggregation of nanofillers.

Author Contributions: The authors have equal contributions. Dmitry V. Pikhurov performed the experiments, Vjacheslav V. Zuev analyzed the data and wrote the paper.

Conflicts of Interest: The authors declare no conflict of interest.

References

1. Bijwe, J.; Logani, C.M.; Tewari, U.S. Influence of fillers and fiber reinforcement on abrasive wear resistance of some polymeric composites. *Wear* **1990**, *138*, 77–92. [CrossRef]
2. Treacy, M.M.J.; Ebesen, T.W.; Gibson, J.M. Nanoparticles as reinforced agents. *Nature (London)* **1996**, *381*, 678–680. [CrossRef]
3. Strobl, G. *The Physics of Polymers*; Springer: Berlin, Germamy, 2007.
4. Maharaj, D.; Bhushan, B. Friction, wear and mechanical behavior of nano-objects on the nanoscale. *Mater. Sci. Eng. R* **2015**, *95*, 1–43. [CrossRef]
5. Troshin, P.; Mukhacheva, O.; Usluer, O.; Goryachev, A.; Akkuratov, A.; Susarova, D. Improved photovoltaic performance of PPV-based copolymers usingoptimized fullerene-based counterparts. *Adv. Energy Mater.* **2013**, *3*, 161–166. [CrossRef]
6. Kasgoz, A.; Akın, D.; Ayten, A.I.; Durmus, A. Effect of different types of carbon fillerson mechanical and rheological properties of cyclic olefin copolymer (COC)composites. *Compos. Part B Eng.* **2014**, *66*, 126–135. [CrossRef]
7. Zhao, L.; Guo, Z.; Cao, Z.; Zhang, T.; Fang, Z.; Peng, M. Thermal and thermo-oxidative degradation of high density polyethylene/fullerene composites. *Polym. Degrad. Stabil.* **2013**, *98*, 1953–1962. [CrossRef]
8. Wan, D.; Wang, Y.; Wen, X.; Qiu, J.; Jiang, Z.; Tan, H. The rheological, thermostable, and mechanical properties of polypropylene/fullerene C60 composites with improved interfacial interaction. *Polym. Eng. Sci.* **2012**, *52*, 1457–1463. [CrossRef]
9. Gocek, I.; Keskin, R.; Ozkoc, G.; Yilmaz, K.; Kamac, Y. Mechanical and electrical properties of polyamide 66 nanocomposites reinforced with Buckminster fullerene C60. In Proceedings of the Fiber Society 2012 Fall Meeting and Technical Conference, Boston, MA, USA, 7–9 November 2012.
10. Naffakh, M.; Diaz-Pascual, A.M.; Marco, C.; Ellis, G.J.; Gomez-Fatou, M.A. Opportunities and challenges in the use of inorganic fullerene-like nanoparticles to produce advanced polymer nanocomposites. *Prog. Polym. Sci.* **2013**, *38*, 1163–1231. [CrossRef]
11. Prato, M. [60] Fullerene chemistry for material science applications. *J. Mater. Chem.* **1997**, *7*, 1097–1109. [CrossRef]
12. Schaefer, D.W.; Justice, R.S. How nano are nanocomposites. *Macromolecules* **2007**, *40*, 8501–8517. [CrossRef]
13. Spitalsky, Z.; Tasis, D.; Papagelis, K.; Galiotis, K. Carbon nanotube–polymer composites: Chemistry, processing, mechanical and electrical properties. *Prog. Polym. Sci.* **2010**, *35*, 357–401. [CrossRef]
14. Moniruzzaman, M.; Winey, K.I. Polymer nanocomposites containing carbon nanotubes. *Macromolecules* **2006**, *39*, 5194–5205. [CrossRef]
15. Zuev, V.V.; Ivanova, Y.G. Mechanical and electrical properties of polyamide-6 based nanocomposites reinforced by fulleroid fillers. *Polym. Eng. Sci.* **2012**, *52*, 1206–1211. [CrossRef]
16. Wang, C.; Guo, Z.-X.; Fu, S.; Wu, W.; Zhu, D. Polymers containing fullerene or carbon nanotube structures. *Prog. Polym. Sci.* **2004**, *29*, 1079–1141. [CrossRef]
17. Zuev, V.V. Polymer nanocomposites containing fullerene C60 nanofillers. *Macromol. Symp.* **2011**, *301*, 157–161. [CrossRef]
18. Bahadur, S. The dewelopment of transfer layers and their role in polymer tribology. *Wear* **2000**, *245*, 92–99. [CrossRef]
19. Gupta, B.K.; Bhushan, B. Fullerene particles as an additive to liquid lubricants and greases for low friction and wear. *Lubr. Eng.* **1994**, *50*, 524–528.

20. Lancaster, J.K. *Polymer Science: A Material Science Handbook*; Jenkins, A.D., Ed.; Noerth Holland: Amsterdam, The Netherlands, 1972.
21. Tewari, U.S.; Bijwe, J.; Mathur, N.J.; Sharma, I. Studies on abrasive wear of carbon fiber (short) reinforced polyamide composites. *Tribol. Int.* **1992**, *25*, 53–60. [CrossRef]
22. Kang, S.C.; Chung, D.W. Improvement of frictional properties and abrasive wear resistance of polyamide/graphite composite by oil impregnation. *Wear* **2003**, *254*, 103–110. [CrossRef]
23. Pozdnykov, A.O.; Kudryvtsev, V.V.; Fridrich, K. Sliding wear of polyimide/fullerene C60 composite coating. *Wear* **2003**, *254*, 501–513. [CrossRef]
24. Franklin, S.E. Wear experiments with selected engineering polymers and polymer composites under dry reciprocating sliding conditions. *Wear* **2001**, *251*, 1591–1598. [CrossRef]
25. Unal, H.; Sen, U.; Mimaroglu, A. Dry wear sliding characteristics of some industrial polymers against steel counterface. *Tribol. Int.* **2004**, *37*, 727–732. [CrossRef]